Inkjet-printed RFID antenna sensor for strain monitoring

C. Cho, X. Yi & Y. Wang
School of Civil and Environmental Engineering, Georgia Institute of Technology, Atlanta, GA, USA

T. Le & M.M. Tentzeris
School of Electrical and Computer Engineering, Georgia Institute of Technology, Atlanta, GA, USA

R.T. Leon
Department of Civil and Environmental Engineering, Virginia Polytechnic Institute and State University, Blacksburg, VA, USA

ABSTRACT: A folded patch antenna has been previously proposed by the authors as a passive wireless sensor for strain and crack sensing. The electromagnetic resonance frequency of the antenna sensor varies correspondingly with physical deformation of the antenna. When the battery-free antenna sensor is bonded on a structural surface, strain and crack can be detected through convenient wireless interrogation. To further reduce sensor production cost, this research investigates inkjet-printing technique for fabricating the antenna sensor. Silver nanoparticles are inkjet-printed on a polyimide thin film to produce the antenna pattern. The printed silver layer replaces copper (as in previous fabrication of antenna sensor) to function as conductor on the antenna. For comparison, antenna sensors are fabricated with different numbers of inkjet-printed layers. To study strain sensing performance, printed antenna sensors are mounted on aluminum specimens for tensile testing. The strain sensing results are compared the previous antenna sensor with copper conductor. Both strain sensitivity and linearity of the printed antenna sensors are similar to previous copper antenna sensor.

1 INTRODUCTION

Determining the integrity of in-service engineering structures is crucial for safe operations. In order to monitor the safety condition of structures, structural health monitoring (SHM) technologies have been investigated and developed (Brownjohn 2007). An SHM system in general integrates processes such as sensing, data transmission, and data processing. To monitor and evaluate structural condition, numerous structural responses can be measured, such as acceleration, deformation, strain, *etc*. Among these structural response data, strain can be one of the most important indicators of structural safety. Many types of sensors can be used to measure strain, e.g. metal foil strain gages, vibrating wire strain gages, and fiber optic sensors. While these strain sensors provide reliable data, they usually entail expensive installation of cables. To reduce the system cost, particularly for application on a large structure, a significant amount of research has been conducted to develop wireless sensor networks for SHM (Lynch and Loh 2006). Each wireless sensor node typically contains sensors, an analog-to-digital converter, a microprocessor with memory for storage and computing, a

wireless radio, and batteries as power supply. Although wireless sensors reduces installation cost, long-term monitoring is still challenging, often due to the short life span of batteries (Straser and Kiremidjian 1998; Lynch *et al.* 2004; Spencer *et al.* 2004; Wang *et al.* 2007).

Eliminating the need of on-board (battery) power supply, a passive wireless folded antenna sensor has been recently developed to measure strain and crack on structures (Yi *et al.* 2011). A folded patch antenna pattern is designed and fabricated. The design consists of three bonded layers, which include the top copper cladding with antenna pattern, the middle layer made of dielectric substrate, and the bottom copper cladding as ground plane. Vias are used to connect top copper cladding with the ground plane to achieve "folding", which reduces the patch antenna size by half. The substrate material sandwiched between the top copper cladding and ground plane is Rogers RT/duroid®5880 (a glass micro-fiber reinforced PTFE material). After attaching the antenna sensor on a base structure that is being monitored, dimensions of the antenna change when strain or crack occurs in the base structure. As a result, the antenna resonance frequency shifts and can be wirelessly interrogated. The antenna sensor utilizes radiofrequency identification (RFID) technology to

achieve wireless data interrogation (Balanis 1997). An off-the-shelf RFID chip, SL3ICS1002 made by NXP Semiconductors, is incorporated with the folded patch antenna. Enabled by the 1mm × 1mm RFID chip, frequency shift of the antenna sensor can be wirelessly modulated and interrogated by a reader. Previously, the antenna sensor is fabricated by milling machines or wet etching techniques. While providing accurate and reliable fabrication quality, these two methods entail expensive production cost (Vyas *et al.* 2011).

To further reduce sensor production cost, this research investigates inkjet-printing techniques for fabricating folded patch antennas. Instead of using copper to conduct electromagnetic current, as in previous fabrication, a thin silver layer is inkjet-printed to replace copper for current conduction. Inkjet-printing technique has been widely adopted for printing RFID temperature sensor, gas sensor, antennas, and other radiofrequency electronics (Shaker *et al.* 2011; Vyas *et al.* 2011). Different inks can be used in printing, such as silver nanoparticles (Merilampi *et al.* 2011) and carbon nanotubes (CNTs) (Occhiuzzi *et al.* 2011).

In this research, silver nanoparticle ink is investigated for inkjet-printing the conductive surface layer of the antenna sensor. To achieve better uniformity in the printed silver, the printing is performed on a flexible and ink-absorbent 5-mil Kapton polyimide film (instead of directly on Rogers RT/duroid® 5880). Bottom of the Kapton thin film is then bonded on a Rogers RT/duroid® 5880 substrate. Compared with previous copper antenna sensors, dimensions of the printed sensor are re-designed to consider the electromagnetic effect of adding the Kapton film. To validate strain sensing performance, the printed antenna sensor is mounted on an aluminum specimen for tensile testing. The strain sensing results of the printed antenna sensor are further compared with the previous copper antenna sensor. The paper is organized as follows. Section 2 reviews the strain sensing mechanism of the RFID antenna sensor. Section 3 first describes the design modification for the printed antenna sensor to accommodate the effect of the 5-mil Kapton HN thin film, and then presents strain sensing simulation results of the printed antenna sensor. Section 4 introduces fabrication procedures of printing, curing, and assembling the printed sensor. Section 5 discusses the tensile test results of the printed patch antenna.

2 STRAIN SENSING MECHANISM OF AN RFID ANTENNA SENSOR

An RFID sensing system generally consists of an RFID reader and an RFID sensor. An RFID sensor contains a small antenna for transmitting and receiving electromagnetic wave, as well as an RFID chip for modulating the electromagnetic wave. The RFID adopted in this research is the SL3ICS1002 model manufactured by NXP Semiconductors. During operation, the RFID reader first emits an interrogation electromagnetic signal to the sensor. If the antenna sensor is within the interrogation range of the reader, some of interrogation power can be captured by the antenna sensor. Once the received power is higher than the turn-on power of the RFID chip, the chip is activated and sends a modulated signal back to the reader. In order to wirelessly activate the antenna sensor, the minimum amount of power transmitted by the reader is defined as the interrogation power threshold. A Tagformance Lite RFID reader (Voyantic Inc. 2011) is adopted for interrogation power threshold measurement. At each frequency point, the reader varies the interrogation power until the power is just enough to activate the RFID chip. After the reader sweeps through the entire frequency range of interest, the interrogation power threshold versus frequency curve can be obtained. The curve reaches its minimum point at antenna resonance frequency. When the antenna sensor deforms due to strain, the antenna resonance frequency changes accordingly. Therefore, strain sensing is achieved utilizing the relationship between antenna resonance frequency and strain. Details of the sensing mechanism and RFID interrogation can be found in Yi *et al* (2011).

3 PRINTED ANTENNA SENSOR DESIGN AND STRAIN SENSING SIMULATION RESULTS

Because the Rogers RT/duroid®5880 substrate (31-mil thickness) is hydrophobic, the substrate surface is not absorbent to silver nanoparticle ink and not suitable for directly printing upon. Therefore, prior to designing the printed antenna sensor, some printing trials are performed. Based upon the trials, Kapton HN thin film with 5-mil thickness is selected as the printing substrate to provide a more absorbent surface to silver ink, so that the printed silver ink layer has acceptable conductivity. The film has a tensile modulus of 370 ksi at room temperature, and provides elongation up to 82% at room temperature. However, because the 5-mil Kapton film is much thinner than the 31-mil Rogers substrate, antenna performance deteriorates if the Kapton film is used
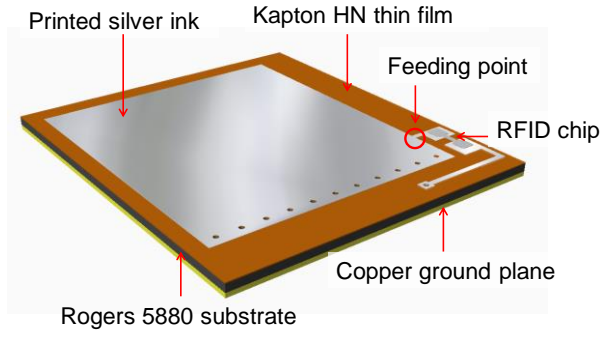
Fig. 1. Drawing of printed antenna sensor (perspective view)

(a) Copper antenna sensor   (b) Printed antenna sensor

Fig. 2. Design modification of the antenna sensor.

to completely replace the Rogers substrate. The performance deterioration includes decrease in both antenna gain and interrogation distance. Furthermore, the Kapton film has a higher relative permittivity (ε_r=3.5) compared with previous Rogers substrate (ε_r=2.2). The higher relative permittivity can also result in larger signal loss. Therefore, the Kapton film is not used to completely replace the Rogers substrate, but rather as the thin film to print upon. To complete the entire antenna sensor with comparable performance as before, the Kapton film printed with silver ink is laid on top of Rogers substrate. Fig. 1 shows that from top to bottom, the four layers of the antenna sensor are the printed silver ink, the 5-mil Kapton HN thin film, 31-mil Rogers RT/duroid®5880 substrate, and the copper ground plane. The manufacturer of the Rogers substrate provides ordering option that allows the substrate to be purchased with a copper layer attached on one side.

Adding a 5-mil Kapton HN film into the original copper antenna sensor (Fig. 2a) changes electromagnetic behavior of the sensor. To continue using RFID interrogation, resonance frequency of the printed antenna sensor needs to maintain at around 915 MHz. The resonance frequency, *f*, of a folded patch antenna can be estimated according to the following equation (Balanis 1997):

$$f \approx \frac{c}{4L\sqrt{\varepsilon_r}} \tag{1}$$

where *c* is the speed of the light, *L* is the length of the top conducting layer, and ε_r is relative permittivity of the substrate. A direct addition of the Kapton HN film into the sensor increases overall relative permittivity of the antenna. According to Eq. (1), to accommodate the permittivity increase, the length of top conducting layer should be reduced. Fig. 2 illustrates design modification of the printed antenna sensor compared to the previous copper antenna sensor. Length of the top conducting layer is re-

duced by 2mm, along with change of matching line and feeding point for impedance matching with the RFID chip. The dimension of the Rogers RT/duroid®5880 substrate remains 61mm×69mm, same as previous copper antenna sensor.
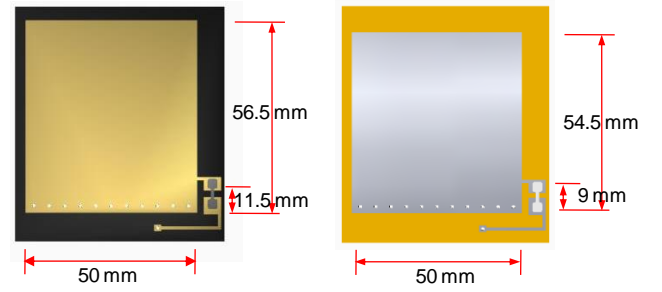
Electromagnetic simulation is conducted using a commercial software package, Ansoft HFSS, to verify the strain sensing performance of the printed antenna. Fig. 3 illustrates the simulation model of the printed antenna sensor. The cubic air box is the domain of the electromagnetic simulation. The outside layer of the air box is assigned as a perfectly matched layer (PML) for absorbing electromagnetic waves coming from the antenna sensor, so that no wave reflects back to the sensor from the PML. The RFID chip is modeled as a lumped port with an impedance of 13.3-j122 Ω, which has the same electrical impedance as the RFID chip made by NXP Semiconductors. Both silver ink and copper material are treated as perfect electrical conductor (PEC) to reduce simulation time. Adaptive mesh method, which increases mesh density until the result converges within a pre-define tolerance, is completed after seventeen iterations at every frequency point and the tetrahedral elements are used in the simulation.

Antenna performance is simulated by sweeping through a frequency range from 900 MHz to 940MHz, at 0.01 MHz step size. To validate the
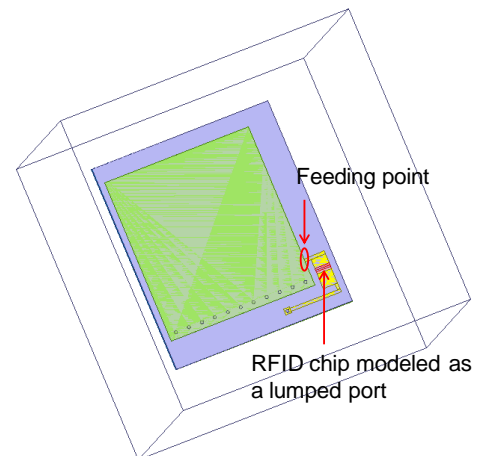
Fig. 3. Simulation model

stain sensing performance through simulation, the printed antenna sensor is deformed from zero strain up to 3,000 με. In this preliminary study, the sensor dimensions are simply scaled according to applied strain. In detail, dimensions along the length of the antenna sensor are increased according to strain, while the dimensions along the width and the thickness are proportionally decreased by Poisson's ratio. Perfect bonding is assumed between different antenna layers, which means no shear lag or strain transfer effect is considered through the thickness direction of the sensor. Scattering parameter (S_{11}) is an important indicator of antenna radiation efficiency at certain frequency. The parameter equals to the ratio of reflected voltage over incident voltage at the lumped port (which models the RFID chip). For the same incident voltage, a lower reflected voltage means more energy is radiated by antenna, i.e. higher radiation efficiency. Therefore, smaller S_{11} value means better matching and higher antenna efficiency. Fig. 4(a) shows S_{11} plots at different strain levels. As expected, the resonance frequency of the printed
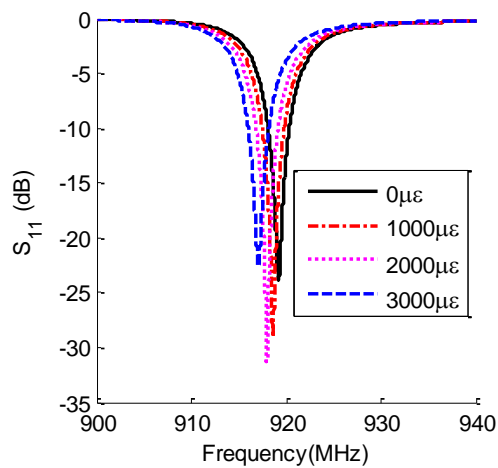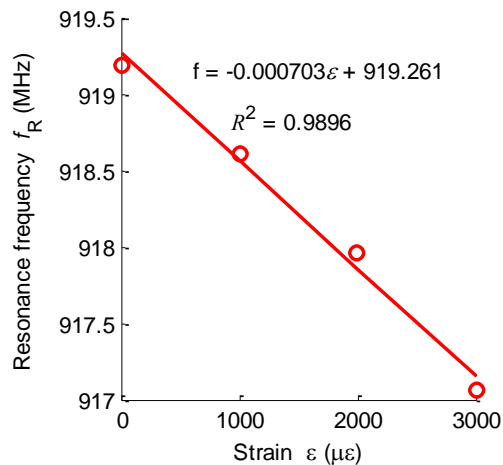
antenna reduces as strain increases. For example, at zero strain level, the resonance frequency is 919.26 MHz, while the resonance frequency decreases to 917.15 MHz at 3,000 με. Fig. 4(b) illustrates linear regression between resonance frequencies and corresponding strain levels. The figure shows the coefficient of determination (R^2) is 0.9896, which indicates a good linearity between resonance frequency and strain. In addition, strain sensitivity is defined as frequency change over strain change:

$$S_\varepsilon = \frac{f_2 - f_1}{\varepsilon_2 - \varepsilon_1} \tag{2}$$

where f_1 is the initial resonance frequency at strain ε_1; f_2 is the resonance frequency at strain ε_2. As shown by linear regression in Fig. 4(b), the strain sensitivity is -703 Hz/με.

4 SENSOR FABRICATION

Early researchers have used a Dimatix Materials printer to inkjet-print silver nanoparticles on various substrate materials to form antennas and other RF electronics (Shaker *et al.* 2011; Vyas *et al.* 2011). The silver nanoparticle ink adopted in this research is Cabot Conductive Ink CCI-300. The Dimatix Materials printer (Fig. 5(a)) uses a cartridge (Fig. 5(b)) to hold the silver nano-particle ink, and is able to print drop sizes of 1pL (pico-Liter) or 10pL onto a smooth, hydrophobic surface. The Cabot Conductive Ink CCI-300, which contains surface modified ultra-fine silver nanoparticles, is engineered for high resolution, low resistivity, and conductive features on a variety of substrates (including Kapton HN thin film).

To achieve high conductivity, the printed silver nanoparticle layer must be cured at 100~150°C, depending on the substrate used. Since the CCI-300 silver nanoparticles have reduced melting and sintering temperatures compared to micro-sized particles, the printed layer can be cured at temperatures as low as 100°C. The curing procedure is important because

(a) S_{11} parameters at different strain levels

(b) Resonance frequency versus strain

Fig. 4. Strain simulation results of the printed antenna sensor in Ansoft HFSS

(a)   (b)

Fig. 5. Printing equipment. (a) Dimatix Materials printer; (b) Cartridge.

the ink needs to be set in high temperature for the particles to create a solid cohesive layer. After curing, the individual silver nanoparticles conglomerate into a solid conductive layer, which is required to provide adequate antenna performance (Vyas *et al.* 2009).

Different printing and curing procedures have also been explored to optimize the antenna performance. In the end, it is decided to print 15 or 20 layers of silver nanoparticles in total on 5-mil Kapton HN thin film. The ink drop size is 1pL, in order to achieve smooth printed surface and a fine printing resolution. Since 15-layer or 20-layer ink is relatively thick for one-time curing, the printed antenna pattern is cured after every 5 layers of printing. With less newly printing layers every time, the curing quality has been improved. During each curing process, the printed ink is cured for 2 hours at 120 °C. The printed antenna pattern is shown in Fig. 6. The printed antenna pattern is bonded with the Rogers RT/duroid® 5880 substrate (thickness of 31 mils) by M-bond 610 glue from Vishay. Holes are punctured through the Kapton HN film at the vias locations of the Rogers substrate. Conductive epoxy from CircuitWorks (CW2460) is then applied inside vias to connect top silver ink printed antenna pattern with the bottom ground plane. In the end, the RFID chip from NXP Semiconductors is soldered to complete the printed antenna sensor.

5 STRAIN SENSING EXPERIMENTS OF THE PRINTED ANTENNA SENSOR

Fig. 7 (a) shows the center area of an aluminum tensile testing specimen, with the printed antenna sensor and seven conventional metal foil strain gages (FLA-2-23-3LT, Texas Measurements, Inc.) measuring the axial strain. Fig. 7 (b) shows the experimental setup for the tensile testing with a 22-kip
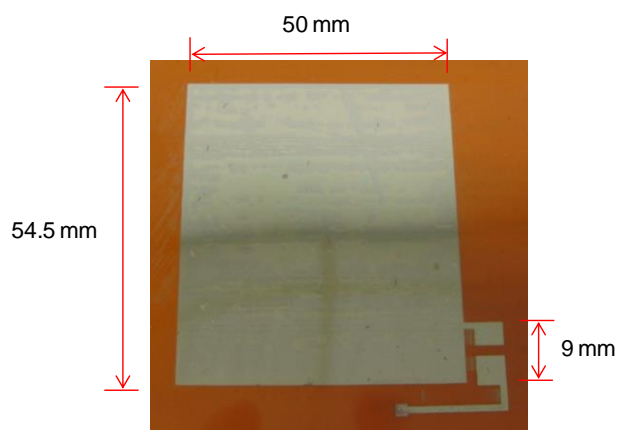
Fig. 6. Photo of the inkjet-printed antenna sensor pattern on Kapton HN material (3in. × 3in.)
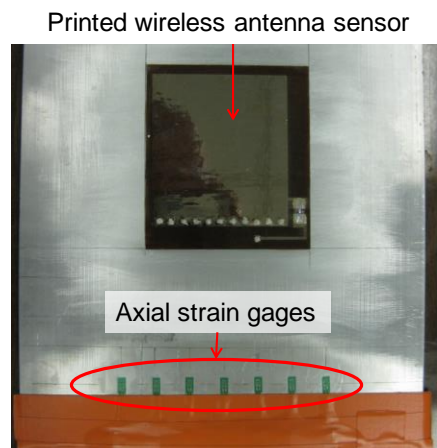
(a) Photo of the sensor instrumentation for wireless sensing experiments
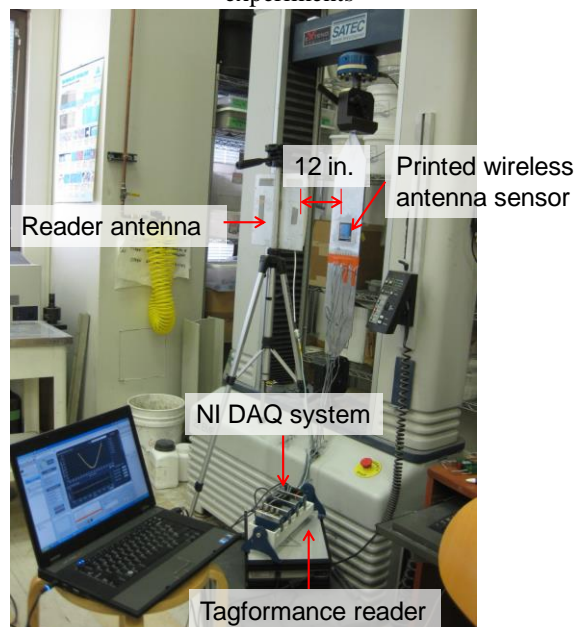
(b) Photo of the wireless strain sensing experiments
Fig. 7. Experimental setup for the tensile tests of printed nanoparticles sensor

SATEC machine. A panel antenna from Cushcraft Corporation (S8658WPC) serves as the reader antenna, which covers a frequency range of 865MHz to 965MHz and has a gain of 8.6 dBi. The reader antenna, which is placed 12 in. away from the center of the printed antenna sensor, is connected with Tagformance Lite reader. The data from metal foil strain gages are collected by National Instruments NI-cDAQ 9172 CompactDAQ Chassis with a NI 9235 strain gage module.

The tensile load applied by the testing machine is configured so that approximately a 50με increment is obtained at each loading step. The interrogation power threshold of the printed antenna sensor is measured by Tagformance Lite reader at each loading step. The applied strain is increased up to around 300με in seven steps. Section 5.1 presents tensile test results of a sensor with 15 layers of printed silver ink. Section 5.2 presents results for a 20-layer printed sensor.

5.1 Sensor with 15 layers of printed ink

Fig. 8(a) plots the average interrogation power threshold against frequency for the printed antenna sensor with 15 layers of silver ink. The strain levels, shown in the legend in Fig. 8(a), are calculated as the average among the seven axial strain gages (in Fig. 7(a)). For clarity, only four representative strain levels are shown in Fig. 8(a). Since the valley area of each plot is relatively flat, the precise resonance frequency is not obvious. To resolve this difficulty, a 4th order polynomial curve fitting is first performed to the valley area of each plot. The value of the fitted 4th order polynomial is re-calculated at a frequency step of 0.001 MHz, in order to identify the resonance frequency at every strain level. The resonance frequency f_R is plotted in Fig. 8(b) against each strain level, showing a measurement sensitivity of -0.000703 MHz/με (i.e. -703 Hz/με). The strain sensitivity matches simulation result, and is also close to the previous copper antenna sensor (Yi *et al.* 2011). In addition, Fig. 8(b) shows the coefficient of determination R^2 from the linear regression. A value of $R^2 = 0.8519$ indicates a lower linearity than pre-vious copper antenna sensor.

5.2 Sensor with 20 layers of printed ink

Since the linearity of the 15-layer printed sensor is relatively low, a 20-layer sensor is printed and tested for performance comparison. Fig. 9(a) presents the interrogation power threshold plots at four repre-sentative strain levels. The interrogation power threshold around the resonance frequency is lower than that in Fig. 8(b), which means that the printed sensor with 20-layer silver ink requires less interro-gation power to turn on the RFID chip. The reason is that the 20-layer silver ink is more conductive than the 15-layer ink. Fig. 9(a) shows the resonance fre-quency of the antenna sensor reduces as the applied strain increases. The resonance frequency at each strain level is extracted and plotted in Fig. 9(b). The strain sensitivity of the 20-layer sensor is -0.000852 MHz/με (i.e. -852 Hz/με), which is higher than the 15-layer sensor presented in Fig. 8(b). The coeffi-cient of determination R^2 of the 20-layer sensor is 0.9175, which is also higher than the 15-layer sen-sor. The improved strain sensitivity and linearity in-
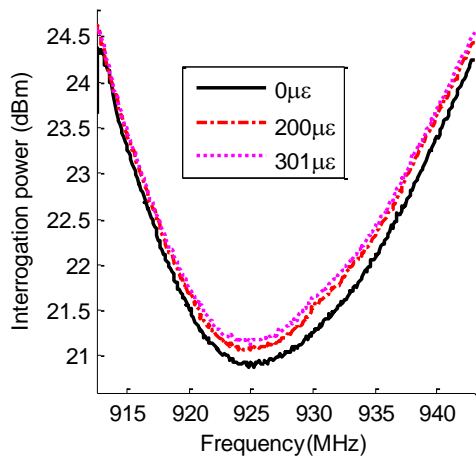
(a) Interrogation power threshold plot at different strain levels
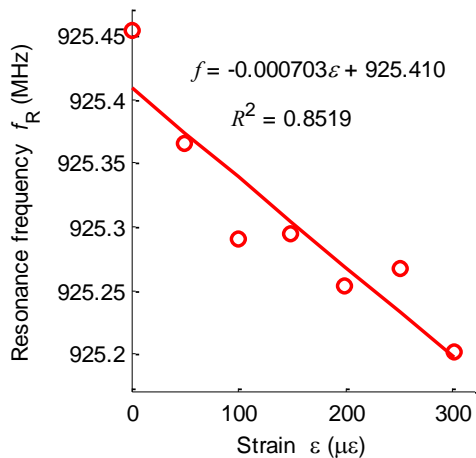
(b) Resonance frequency change versus strain relationship

Fig. 8. Strain sensing results of 15-layer printed sensor
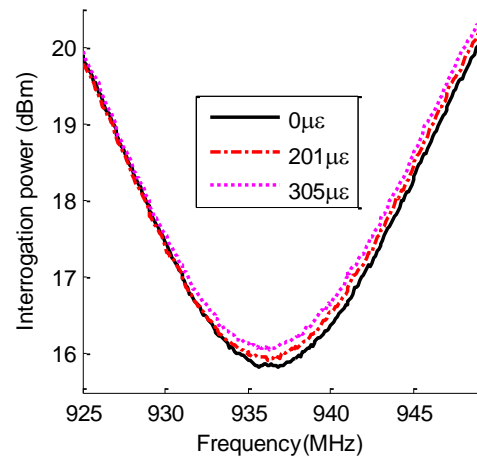
(a) Interrogation power threshold plots under different strain levels
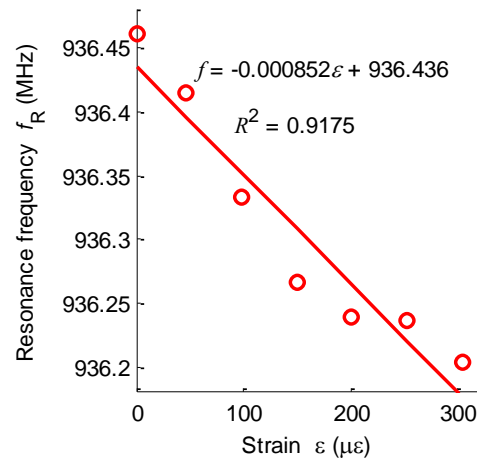
(b) Resonance frequency change versus strain relationship

Fig. 9. Strain sensing results of 20-layer printed sensor

dicate that the sensor performance is better with 20-layer fabrication. Nevertheless, the linearity of the 20-layer fabrication is still relatively low compared with previous copper antenna sensor.

6 CONCLUSIONS

This paper presents a passive RFID antenna sensor made through inkjet-printing of silver nanoparticle ink. In previous research, although a copper antenna sensor shows good performance for strain and crack sensing, the sensor fabrication cost is relatively high. To lower fabrication cost, this research investigates inkjet printing technique for sensor fabrication. Silver nanoparticle ink is printed on a Kapton polyimide thin film to form the conducting layers of the antenna pattern. First, the copper antenna sensor is redesigned by integrating 5-mil Kapton HN thin film into the sensor. Strain sensing performance of the printed antenna sensor is then validated through numerical simulation. For experimental validation, two sensors are fabricated, one with 15-layer printing and the other with 20 layers. Both sensors are tested for strain sensing. The tensile test results show that the measured strain sensitivities are close to simulation results. The strain sensing linearity of the 20-layer sensor is higher than the 15-layer sensor, which indicates that the printed sensor performance can be improved by increasing the number of printed silver ink layers. Meanwhile, the strain sensitivity of the printed antenna sensor is also similar as the previous copper patch antenna sensor. Future work is needed to improve the strain sensing linearity of the printed sensor. The footprint of the copper antenna sensor will be further reduced by implementing miniaturization techniques.

7 ACKNOWLEDGEMENT

8 REFERENCES

Balanis, C. A. 1997. *Antenna Theory: Analysis and Design*. John Wiley & Sons, New York.

Brownjohn, J. M. W. 2007. Structural health monitoring of civil infrastructure. *Philosophical Transactions of the Royal Society A: Mathematical, Physical and Engineering Sciences* 365(1851): 589-622.

Lynch, J. P., K. H. Law, A. S. Kiremidjian, C. E., C. R. Farrar, H. Sohn, D. W. Allen, B. Nadler and J. R. Wait 2004. Design and performance validation of a wireless sensing unit for structural health monitoring applications. *Structural Engineering and Mechanics* 17: 393-408.

Lynch, J. P. and K. J. Loh 2006. A summary review of wireless sensors and sensor networks for structural health monitoring. *The Shock and Vibration Digest* 38(2): 91-128.

Merilampi, S., T. Bjorninen, U. Leena, P. Ruuskanen and L. Sydanheimo 2011. Embedded wireless strain sensors based on printed RFID tag. *Sensor Review* 31(1): 32-40.

Occhiuzzi, C., A. Rida, G. Marrocco and M. M. Tentzeris 2011. RFID passive gas sensor integrating carbon nanotubes. *IEEE Transactions on Microwave Theory and Techniques* 59(10): 2674-2684.

Shaker, G., S. Safavi-Naeini, N. Sangary and M. M. Tentzeris 2011. Inkjet printing of ultrawideband (UWB) antennas on paper-based substrates. *IEEE Antennas and Wireless Propagation Letters* 10: 111-114.

Spencer, B. F., Jr., M. E. Ruiz-Sandoval and N. Kurata 2004. Smart sensing technology: opportunities and challenges. *Structural Control and Health Monitoring* 11(4): 349-368.

Straser, E. G. and A. S. Kiremidjian 1998. *A Modular, Wireless Damage Monitoring System for Structures*. John A. Blume Earthquake Eng. Ctr., Stanford University, Stanford, CA Report No. 128.

Voyantic Inc. 2011. *Tagformance Measurement System Manual*. Voyantic Inc., Espoo, Finland

Vyas, R., V. Lakafosis, H. Lee, G. Shaker, L. Yang, G. Orecchini, A. Traille, M. M. Tentzeris and L. Roselli 2011. Inkjet printed, self powered, wireless sensors for environmental, gas, and authentication-based sensing. *IEEE Sensors Journal* 11(12): 3139-3152.

Vyas, R., V. Lakafosis, A. Rida, N. Chaisilwattana, S. Travis, J. Pan and M. M. Tentzeris 2009. Paper-based RFID-enabled wireless platforms for sensing applications. *IEEE Transactions on Microwave Theory and Techniques* 57(5): 1370-1382.

Wang, Y., J. P. Lynch and K. H. Law 2007. A wireless structural health monitoring system with multithreaded sensing devices: design and validation. *Structure and Infrastructure Engineering* 3(2): 103-120.

Yi, X., T. Wu, Y. Wang, R. T. Leon, M. M. Tentzeris and G. Lantz 2011. Passive wireless smart-skin sensor using RFID-based folded patch antennas. *International Journal of Smart and Nano Materials* 2(1): 22-38.